

X-691-73-372

PREPRINT

NASA TM X-70543

# ANGULAR DISTRIBUTIONS AND POLARIZATION FRACTIONS OF HELIUM RESONANCE RADIATION ( $n^1 P - 1^1 S$ ) IN THE EXTREME ULTRAVIOLET

M. J. MUMMA  
M. MISAKIAN  
W. M. JACKSON  
J. L. FARIS

DECEMBER 1973

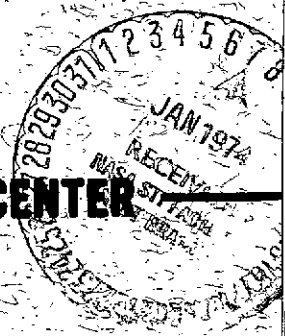
ANGULAR DISTRIBUTIONS AND POLARIZATION FRACTIONS OF HELIUM RESONANCE RADIATION ( $n^1 P - 1^1 S$ ) IN THE EXTREME ULTRAVIOLET (NASA) 33 p HC \$3.75

CSCCL 20H G3/24

Unclas 24654



GODDARD SPACE FLIGHT CENTER  
GREENBELT, MARYLAND



ANGULAR DISTRIBUTIONS AND POLARIZATION FRACTIONS OF  
HELIUM RESONANCE RADIATION ( $n^1P - 1^1S$ ) IN  
THE EXTREME ULTRAVIOLET

M. J. Mumma  
M. Misakian\*  
W. M. Jackson  
J. L. Faris

Laboratory for Extraterrestrial Physics  
NASA/Goddard Space Flight Center  
Greenbelt, Maryland 20771

\*NAS-NRC Postdoctoral Research Associate. Present address:  
Institute of Fluid Dynamics and Applied Mathematics,  
University of Maryland, College Park, Maryland 20742

## ABSTRACT

We present the first experimentally determined angular intensity distributions of helium ( $n^1P - 1^1S$ ) resonance photons with respect to the exciting electron beam. The angular intensity distributions were measured at selected electron impact energies from 25 eV (near threshold) to 150 eV. Polarization fractions ( $\Pi$ ) were obtained by analyzing the data in terms of the theoretical relation between angular intensity distribution and  $\Pi$ , i.e.  $I(\theta) = I(90) (1 - \Pi \cos^2 \theta)$ . The experimental values for  $\Pi$  are compared with recent theoretical results and with previous experimental values for the ( $3^1P - 2^1S$ ) transition. Our results are slightly higher than the theoretical results for electron impact energies from 80 eV to 150 eV, e.g. 0.36 vs 0.32 at 100 eV. Our values for  $\Pi$  reach a maximum at  $\sim 40$  eV where  $\Pi = 0.55$  and then decrease for lower electron energies, reflecting the increasing importance of cascade ( $m^1S - n^1P$ ) transitions at lower electron energies.

ANGULAR DISTRIBUTIONS AND POLARIZATION FRACTIONS OF  
HELIUM RESONANCE RADIATION ( $n^1P - 1^1S$ ) IN  
THE EXTREME ULTRAVIOLET

M. J. Mumma  
M. Misakian \*  
W. M. Jackson  
J. L. Faris

Laboratory for Extraterrestrial Physics  
NASA/Goddard Space Flight Center  
Greenbelt, Maryland 20771

ABSTRACT

We present the first experimentally determined angular intensity distributions of helium ( $n^1P - 1^1S$ ) resonance photons with respect to the exciting electron beam. The angular intensity distributions were measured at selected electron impact energies from 25 eV (near threshold) to 150 eV. Polarization fractions ( $\Pi$ ) were obtained by analyzing the data in terms of the theoretical relation between angular intensity distribution and  $\Pi$ , i.e.  $I(\theta) = I(90) (1 - \Pi \cos^2 \theta)$ . The experimental values for  $\Pi$  are compared with recent theoretical results and with previous experimental values for the ( $3^1P - 2^1S$ ) transition. Our results are slightly higher than the theoretical results for electron impact energies from 80 eV to 150 eV, e.g.

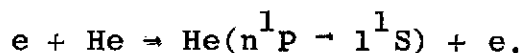
---

\*NAS-NRC Postdoctoral Research Associate. Present address:  
Institute of Fluid Dynamics and Applied Mathematics, University  
of Maryland, College Park, Md. 20742

0.36 vs 0.32 at 100 eV. Our values for  $\Pi$  reach a maximum at  $\sim 40$  eV where  $\Pi = 0.55$  and then decrease for lower electron energies, reflecting the increasing importance of cascade ( $m^1S - n^1P$ ) transitions at lower electron energies.

## INTRODUCTION

The polarization of visible light emissions from helium following electron impact has been the subject of many experimental studies over the past 40 years.<sup>1</sup> All of these earlier studies dealt with transitions between energy states with high principal quantum numbers ( $n$ ). The lower states of the transitions had  $n \geq 2$  and thus the emitted photons were in the visible region of the spectrum. There have been no measurements of polarization fractions for photons emitted in transitions to the ground state ( $1^1S$ ) because those photons lie in the extreme ultraviolet (XUV) spectral region where polarization measurements are difficult. However, recent theoretical calculations<sup>2</sup>, which are based on accurate helium wave functions and the Born approximation, suggest that the polarization fractions for photons emitted in the transitions ( $n^1P - 1^1S$ ) are almost independent of  $n$ . This in turn suggests that the correctness of the predicted dependence of polarization fractions on the electron impact energy can be checked experimentally in a simple way. We present here the first measurements of polarization fractions ( $\Pi$ ) for XUV photons from helium via the process



The results are compared with theory and with experimental polarization fractions for ( $3^1P - 2^1S$ ) radiation. Measurements of  $\Pi$  were made for incident electron energies ranging in value from 25 eV (near threshold), where cascade effects and negative ion resonances appear to play an important role, to 150 eV where a comparison is made with predictions of the Born theory.

#### THEORY AND EXPERIMENT

The origin of the polarization of helium resonance radiation following electron impact excitation is reviewed in the following simple discussion.<sup>3</sup> Consider a pencil beam of electrons having cylindrical symmetry and passing through a Maxwellian gas of helium atoms. The direction of the incident electron beam defines the z-axis, the y-axis is taken to be the line joining the center of the interaction region and the position of the detector at  $\theta = 90^\circ$  with respect to the electron beam, and the x-axis completes the orthogonal system (Fig. 1).

Excitation of the  $n^1P$  levels by monoenergetic electron impact on He ( $1^1S$ ) will in general populate the hyperfine levels ( $m = 0, \pm 1$ ) in an unequal way and this leads to anisotropy in the emitted radiation pattern. The intensity

pattern can be described in terms of three mutually orthogonal electric dipoles ( $p_x, p_y, p_z$ ) where  $p_x = p_y = P_{\perp}$  (the electron beam direction is an axis of cylindrical symmetry) and  $P_z = P_{\parallel}$ . The expectation value,  $\langle P_j \rangle$ , for the  $j$ th component of the electric dipole matrix element is related to the selection rules for  $\Delta m$  in the standard way,

$$\langle P_j \rangle = \int (\Psi_{\ell}^m)^* x_j (\Psi_{\ell}^m) d\tau \quad (2)$$

where  $\Psi_{\ell}^m$  represents the helium atom wave functions and  $d\tau$  is a differential volume element in spherical coordinates. Integration over the  $\phi$  coordinate yields the selection rules

$$\left. \begin{aligned} \langle P_z \rangle &= 0 \quad \text{unless } \Delta m = 0, \\ \langle P_x \rangle &= 0 \\ \langle P_y \rangle &= 0 \end{aligned} \right\} \text{unless } \Delta m = \pm 1. \quad (3)$$

The intensity of radiation in the direction of the  $y$ -axis is then given by

$$I(90) = I_{\parallel} + I_{\perp}, \quad (4)$$

where  $I_{\perp}$  is the intensity contribution from  $P_x$  and  $I_{\parallel}$  is the intensity contribution from  $P_z$ . The intensity at any other angle,  $I(\theta)$ , is

$$I(\theta) = I_{\parallel} \sin^2 \theta + I_{\perp} (1 + \cos^2 \theta). \quad (5)$$



Eqn. (5) can be rearranged to read

$$I(\theta) = I(90) \left\{ 1 - \Pi \cos^2 \theta \right\}, \quad (6)$$

where

$$\Pi = (I_{\parallel} - I_{\perp}) / (I_{\parallel} + I_{\perp}). \quad (7)$$

$\Pi$  is called the polarization fraction.

The polarization fraction can be obtained theoretically by calculating the excitation cross sections for the hyperfine levels ( $m$ ) at a particular electron impact energy. Vriens and Carriere have recently reported the results of such a calculation for electron impact and for proton impact in helium<sup>2,4</sup>.

The polarization fraction can be determined experimentally from measurements of the angular intensity dependence of radiation for a given wavelength using Eqn. 6. This method was apparently first used by Smit<sup>5</sup> in an attempt to measure the polarization fractions of visible radiation from helium. The approach used by most investigators has been to measure  $I_{\parallel}$  and  $I_{\perp}$  of a particular resonance line at 90 degrees with respect to the electron beam using a polarizer-monochromator arrangement. This procedure is prone to error, however, if proper allowance is not made for the polarizing effects of the

measuring instruments<sup>6</sup>. We will return to this point later when comparing our data with the measurements of other workers.

The theoretical results of Vriens and Carriere<sup>2</sup> suggest that it is not necessary to isolate the individual resonance lines ( $n^1P - 1^1S$ ) in order to determine the polarization fractions since the values for  $\Pi$  are only weakly dependent on "n" (Table 1). Furthermore, the excitation cross sections fall off rapidly with increasing "n" so that only the lowest few levels ( $n \leq 4$ ) contribute significantly to the total intensity<sup>7</sup>. XUV radiation from excited states of  $He^+$  makes only a small contribution to the total intensity. For 150 eV electrons, roughly 5% of the total radiation measured<sup>7,8</sup> is produced from excited  $He^+$  ( $2^2P \rightarrow 1^2S$ , 303 Å;  $3^2P \rightarrow 1^2S$ , 256 Å; and  $He^+$  ( $4 \rightarrow 2$ ), 1215 Å). This percentage decreases as the electron energy is lowered. These considerations suggest that the polarization fractions of the resonance lines can be determined from measurements of the angular distribution of the XUV radiation emitted following electron impact on helium. During the present study, the angular intensity distribution,  $I(\theta)$ , of the XUV photons was measured with respect to the electron beam direction and the polarization fraction was determined from Eqn. 6.

A schematic view of the apparatus is shown in Fig. 2. An approximately monoenergetic ( $\sim 0.4$  eV spread, FWHM), pulsed, electrostatically focussed electron beam traversed a scattering cell ( $\sim 1.6$  cm radius) filled with helium gas. The cell pressure was measured with an MKS Baratron and was typically  $\sim 10^{-5}$  torr. The partial pressure of helium outside the cell was less than  $\sim 1 \times 10^{-6}$  torr. A plot of photon counts versus cell pressure was linear indicating that radiation trapping was not significant. Inelastic electron collisions with the gas produced helium resonance photons ( $n^1P - 1^1S$ ) and metastable He( $^3S, ^1S$ ) atoms which then passed through a collimating slit system and were detected with a brass metal surface located 20.5 cm away in the field of view of a continuous electron multiplier ("Channeltron", Electro-Optics Division, Bendix Co.). Transitions between excited S and P states in the triplet manifold yielded photons in the infrared and visible (see Fig. 3) and were not observed because of insufficient energy to produce Auger electrons at the metal surface detector; only transitions to the ground state provide photons with enough energy ( $E \gtrsim 7$  eV;  $\lambda \lesssim 1800\text{\AA}$ ) to be detected. Time-of-flight techniques were used to separate the photon signal from the metastable atoms. Ions and scattered

electrons were removed by electrostatic deflection plates. The angular intensity distribution of XUV He resonance radiation was measured by rotating the electron gun-collision cell-electron collector assembly with respect to the detector. The angle  $\theta$  could be varied from 40 to 140 degrees with respect to the electron beam direction. The field of view was  $< 2$  degrees and the angle could be set to within 0.1 degree.

The apparatus was first tested by measuring the angular intensity distribution of the  $\text{OI}(^3\text{P} - ^3\text{S})$  resonance multiplet at  $1304 \text{ \AA}$ . This multiplet was excited by dissociative excitation of  $\text{O}_2$  with 100 eV electrons. A  $\text{CaF}_2$  window was placed in front of the detector for this measurement in order to restrict the photon bandpass from  $\sim 1250 \text{ \AA}$  to  $\sim 1800 \text{ \AA}$ . The only strong emission feature which can be excited in this wavelength range by electron impact on  $\text{O}_2$  is the  $\text{OI}(1304 \text{ \AA})$  multiplet<sup>9</sup>. Theoretically, we expect the photons of the  $\text{OI}(1304 \text{ \AA})$  multiplet to have an isotropic angular distribution since the upper state has  $L = 0$ . Our measured angular distribution (Fig. 4) was isotropic ( $40^\circ \leq \theta \leq 140^\circ$ ) to within experimental error (a few percent) in agreement with theory.

We next measured the angular dependence of the XUV He

resonance photons with the  $\text{CaF}_2$  window removed. Data were taken in the forward and backward quadrants at angles symmetric with respect to  $90^\circ$ . Six or more intensity measurements were made at  $90$  degrees and two or more measurements were made for each of the other angles. During some experimental runs, the set of angles chosen were  $\{40,50,70,90,110,130,140\}$  degrees while on other runs, the angles were  $\{40,60,90,120,140\}$  degrees. The data,  $I(\theta)$ , were analyzed by plotting  $I(\theta)/I(90)$  vs  $\cos^2 \theta$  and determining the slope (polarization fraction),  $\Pi$ , of the linear relation given by Eqn. 6 using a least square method (see Fig. 5). The experimental values for  $\Pi$  as a function of electron energy are listed in Table II and shown in Fig. 6. The broken curve is an approximate fit to the experimental data and the solid curve is from a calculation by Vriens and Carriere<sup>2</sup> based on the Born theory and the generalized oscillator strengths of Kim and Inokuti<sup>10</sup>. Because photons from the  $n = 2,3$  and 4 states were simultaneously detected (contributions from  $n > 4$  are expected to be less than a few percent) and their respective polarization fractions are slightly different<sup>2</sup>, the theoretical curve shown in Fig. 5 has been weighted accordingly<sup>11</sup>. The relative contributions from the  $n = 2,3$  and 4 states were determined using the excitation cross sections of Donaldson,

Hender and McConkey<sup>7</sup>. Corrections for cascade effects have not been made but such effects are not expected to be large at higher electron energies. For example, the population of the  $2^1P$  state is expected to be increased roughly by 10% for 100 eV electrons due to cascade contributions from  $n^1S$  and  $n^1D$  ( $n > 2$ ) states<sup>8</sup>. The impact of this on the polarization fraction for  $2^1P - 1^1S$  radiation should be reduced since the various  $2^1P$  magnetic sublevels will each receive cascade contributions. As the incident electron energy is decreased, the relative contributions from cascade processes increase<sup>8</sup> and we would expect to see some lowering in the value of  $\Pi$  for a given emission line; this is discussed further below. It can be seen from Fig. 6 that our results at higher electron energies are somewhat greater than the theoretical predictions, the ratio being about 1.12 at 100 eV (i.e. 0.32 from theory vs. 0.36 from experiment).

A comparison of our data with the polarization fractions measured by other workers is shown in Fig. 7. Because no earlier measurements in the XUV exist, we have presented the results for the  $3^1P - 2^1S$  transition which radiates at 5016Å. We take advantage of the fact<sup>2</sup>, as have earlier investigators,<sup>12,13</sup> that the behavior of  $\Pi$  for electron energies well above threshold is nearly independent of the principal quantum number  $n$ . Thus

the hyperfine levels of the  $2^1P$  and  $3^1P$  states will be populated in almost the same way and radiation to  $L = 0$  states should yield the same polarization fraction for the respective multiplets. The work of Heddle and Lucas<sup>14</sup> agrees well with the present results for low electron energies but a comparison becomes more difficult at higher energies because of the scatter in their data. We note that their measurements have been made at right angles to the electron beam with a linear polarizer-quartz prism monochromator combination. Compensation for different monochromator sensitivity for  $I_{||}$  and  $I_{\perp}$  was made by using a tilted silica plate following the polarizer.

Agreement with the data of Moussa et. al.<sup>12</sup> and Van Eck and De Jongh<sup>13</sup> is not satisfactory, however. Their values for  $\Pi$  are nearly a factor of two smaller than the present measurements. Their results are, apparently fortuitously, in good agreement with the predictions for excitation by proton impact<sup>15</sup>. The large discrepancy between Heddle's and our study and the data of references 12 and 13 has no clear explanation. Van Eck and De Jongh have attempted to correct for different sensitivity of their monochromator for light polarized parallel and perpendicular to the rulings of their grating by setting  $I_{||} = I_{\perp}$  for light observed at 270 eV. While this equality

between  $I_{\parallel}$  and  $I_{\perp}$  at 270 eV is satisfied according to the theoretical predictions assuming proton excitation of helium, it is incorrect for electron excitation<sup>2</sup>. An estimate of the error introduced into their results cannot be made here, however, because their unreduced intensity data were not published.

Moussa et.al. corrected for the polarization effects of their grating monochromator by first measuring the relative intensities  $k_{\parallel}(\lambda)$  and  $k_{\perp}(\lambda)$  using an argon-filled tungsten ribbon lamp and a polarizer. The relatively poor agreement of their data with theory, however, suggests that their calibration procedure should be reexamined.

Examining our polarization data at low electron energies, we observe a "folding over" for values of  $\Pi$ . This effect has been previously observed near threshold for the He( $3^1P - 2^1S$ ) transition<sup>14,16</sup>. Simple arguments of momentum conservation show that  $\Pi$  goes to unity at threshold<sup>17</sup>. Until recently, it had been thought that  $\Pi$  would increase monotonically as the electron energy was decreased to threshold. However, as we have noted above, the relative cascade contributions to the  $n^1P$  states become larger as the incident electron energy is lowered. For 30 eV electrons, roughly 30% of the radiation from the  $2^1P - 1^1S$



transition arises from cascade contributions to the  $2^1P$  state<sup>8</sup>. As the various magnetic sublevels of the  $2^1P$  state will each receive contributions, we would expect to see some lowering in the value of  $\Pi$ . The calculations of Burke et.al.<sup>18</sup> have demonstrated how the presence of helium negative ion resonances<sup>19</sup> close to the  $2^1P$  threshold can strongly influence the value of  $\Pi$  when the electron energy is within a few eV of threshold. An estimate of the near threshold behavior of  $\Pi(2^1P - 1^1S)$  calculated by Burke et.al. is shown in Fig. 7. As the electron energy is increased above the  $2^1P$  threshold, the value of  $\Pi$  is expected to drop sharply to a minimum and then rise to a secondary maximum. Such a sharp drop near threshold for the  $3^1P \Rightarrow 2^1S$  transition has been observed experimentally.<sup>16,20</sup> The secondary maximum evidently occurs in the present case near 40 eV (Fig. 6).

#### CONCLUSION

We have presented the first measurements of polarization fraction for XUV resonance photons from helium following electron impact by measuring the angular distribution of the  $(n^1P - 1^1S)$  radiation. The technique of determining  $\Pi$  by examining the angular distribution of photons has the advantage that no

instrumental polarization is introduced into the data. The near agreement of our results with theory at high electron energies (80 - 150 eV) and observation of the expected qualitative behavior at low electron energies provides further support for the correctness of the approach.

## REFERENCES

1. The many investigations include K. Steiner, Z. Phys. 52, 516 (1928); W.E. Lamb and T.H. Maiman, Phys. Rev. 105, 573 (1957); R.H. McFarland and E.A. Soltysik, Phys. Rev. 127, 2090 (1962); R.H. Hughes, R.B. Kay and L.D. Weaver, Phys. Rev. 129, 1630 (1963); H.G.M. Heideman, C. Smit and J.A. Smit, Physica 45, 305 (1969). Still other studies are among the references cited below.
2. L. Vriens and J.D. Carriere, Physica 49, 517 (1970).
3. Though portions of the brief discussion that follows can be found elsewhere (for example, L. Harris and A.L. Loeb, Introduction to Wave Mechanics, McGraw Hill (1963) and Ref. 5), the material is presented here for the convenience of the reader.
4. See J. Vanden Bos, Physica 42, 245 (1969) for an earlier calculation of polarization fractions following proton impact on helium.
5. J.A. Smit, Physica 2, 104 (1935). Smit's early results were inaccurate due to limitations of his apparatus. More recently McFarland and Soltysik (Phys. Rev. 129, 2581 (1963)) used the angular distribution method with some success to measure polarization fractions of the 4922 Å ( $4^1D \rightarrow 2^1P$ ) line of helium.

6. D. Clarke and J.F. Grainger, Polarized Light and Optical Equipment, Pergamon Press (1971).
7. F.G. Donaldson, M.A. Hender and J.W. McConkey, J. Phys. B 5, 1192 (1972).
8. L.J. Kieffer, JILA Information Center Report #7, "Compilation of Low Energy Electron Collision Cross Section Data, Part II", (Sept., 1969).
9. M.J. Mumma and E.C. Zipf, J. Chem. Phys. 55, 1661 (1971).
10. Y-K. Kim and M. Inokuti, Phys. Rev. 175, 176 (1968); 181, 205 (1969); 184, 38 (1969).

11. Using Eqn. 6, it can be shown that the total light intensity  $I_t$  is  $I_t = 4\pi I(90)(1 - \Pi_t/3)$ . Solving for  $\Pi_t$ ,  $\Pi_t = 3(1 - I_t/4\pi I(90))$ . Using this relation and taking  $I = k\sigma$  where sigma is an excitation cross section and  $k$  is a proportionality constant and the relation  $I(90) = I(90)_2 + I(90)_3 + I(90)_4$ , it can be shown that  $\Pi_t = 3(1 - M^{-1})$  where

$$M = \frac{\sigma_2}{(1 - \Pi_2/3)} + \frac{\sigma_3}{(1 - \Pi_3/3)} + \frac{\sigma_4}{(1 - \Pi_4/3)}$$

where  $\Pi_2$ ,  $\Pi_3$  and  $\Pi_4$  are polarization fractions for  $n^1P - 1^1S$  transitions for  $n = 2, 3$  and  $4$ . The cross sections

$\sigma_2, \sigma_3$ , and  $\sigma_4$  are for excitation to the  $n = 2, 3$  and  $4$  singlet P states in helium. We note that the values of  $\Pi_t$ , as a function of electron energy, will be close to  $\Pi_2$  because over 70% of the XUV photons are produced by the He ( $2^1P - 1^1S$ ) transition (Ref. 7) for electron energies from 30 to 150 eV.

12. H.R.M. Moussa, F.J. DeHeer and J. Schutten, *Physica* 40, 517 (1969).
13. J. Van Eck and J.P. DeJongh, *Physica* 47, 141 (1970).
14. D.W.O. Heddle and C.B. Lucas, *Proc. Roy. Soc. (London)* A271, 129 (1963).
15. References 12 and 13 assumed that the electron cross sections (and thus the values of  $\Pi$ ) could be determined from the proton cross section theory (Ref. 4) by comparing projectiles of equal velocity. The calculations of Vriens and Carriere (Ref. 2) have shown that this procedure is valid only at very high electron energies (i.e.  $E_{el} > 1000$  eV).
16. R.H. McFarland, *Phys. Rev.* 133, A986, (1964).
17. W.E. Lamb, *Phys. Rev.* 105, 559 (1957).

18. P.G. Bruke, J.W. Cooper and S. Ormonde, Phys. Rev. 183, 245 (1969).
19. For a brief listing of negative ion resonance studies in helium, see H.G.M. Heideman, W. Van Dalfsen and C. Smit, Physica 51, 215 (1971).
20. D.W.O. Heddle and R.G.W. Keesing, Proc. Roy. Soc. (London) A299, 212 (1967) and E.A. Soltysik, A.Y. Fournier and R.L. Gray, Phys. Rev. 153, 152 (1967). The near threshold behavior of  $\pi$  for the  $3^1P \rightarrow 2^1S$  and  $2^1P \rightarrow 1^1S$  transitions may be similar because negative ion resonances are also expected near the higher ( $n > 2$ ) excited states of helium (C. Smit, H.G.M. Heideman and J.A. Smit, Physica 29, 245 (1963)).

TABLE 1

DEPENDENCE OF  $\Pi$  ON ELECTRON ENERGY AND  
PRINCIPAL QUANTUM NUMBER  $n$  AFTER REF. 2.

<u>E(eV)</u>	<u><math>\Pi(2^1P)</math></u>	<u><math>\Pi(3^1P)</math></u>	<u><math>\Pi(4^1P)</math></u>
80	.399	.419	.425
100	.326	.342	.347
150	.204	.215	.218
200	.128	.135	.137

TABLE II

VARIATION OF  $\Pi$  WITH ELECTRON ENERGY

<u>Electron Energy</u>	<u>Trial</u>		
	1	2	3
25	0.42 $\pm$ .05	0.37 $\pm$ .06	
30	0.50 $\pm$ .02	0.48 $\pm$ .02	
35	0.59 $\pm$ .03	0.55 $\pm$ .03	0.54 $\pm$ .03
40	0.51 $\pm$ .03	0.55 $\pm$ .02	0.53 $\pm$ .03
45	0.53 $\pm$ .03	0.53 $\pm$ .02	
49	0.54 $\pm$ .02		
50	0.52 $\pm$ .02		
55	0.50 $\pm$ .02		
60	0.49 $\pm$ .02		
65	0.50 $\pm$ .02		
80	0.40 $\pm$ .02	0.44 $\pm$ .02	0.38 $\pm$ .02
100	0.39 $\pm$ .02	0.35 $\pm$ .02	0.36 $\pm$ .02
101	0.37 $\pm$ .03		
150	0.26 $\pm$ .02		



## FIGURE CAPTIONS

Fig. 1 - Angular dependence of dipole radiation.

Fig. 2 - Schematic view of apparatus.

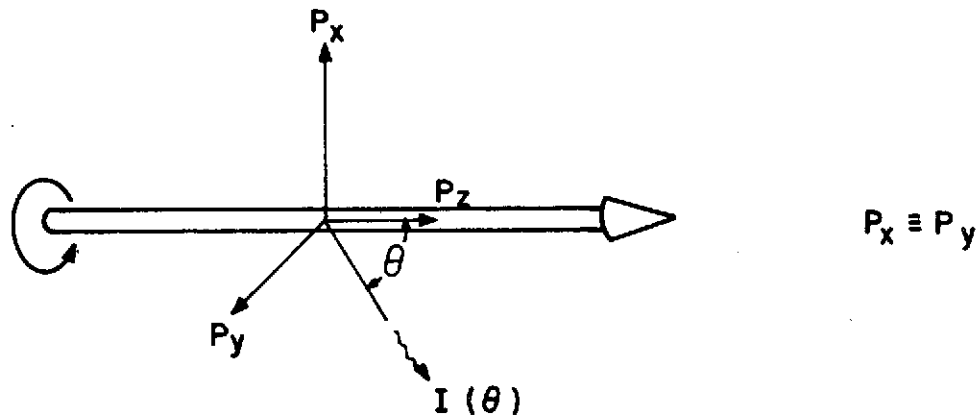
Fig. 3 - Level diagram for neutral helium. The observable radiation originated primarily from ( $n^1P - 1^1S$ ,  $n \geq 2$ ) transitions. Excited states of  $He^+$  yielded only a small percentage of XUV photons at higher electron energies.

Fig. 4 - Angular dependence of  $OI(1304\text{\AA})$  multiplet by 100 eV electrons impacting on  $O_2$ .

Fig. 5 - The points shown are average values of raw data measured in the forward and backward quadrants after multiplication by  $\sin \theta$  to correct for change in the interaction volume viewed by the detector. The values of the slope ( $\pi$ ) and standard deviation are obtained using a least squares fitting procedure employing all the raw data points.

Fig. 6 - The polarization fraction,  $\pi$ , is plotted as a function of electron energy. The error bars shown represent the standard deviation of  $\pi$  using the least squares fitting procedure.

Fig. 7 - Comparison of present results with theory and  
earlier experiments.



STANDARD DIPOLE RADIATION FORMULA :

$$I(\theta) \propto P_i^2 \sin^2 \theta$$

ANGULAR INTENSITY DISTRIBUTION FOR GENERAL CASE :

$$I(\theta) \propto P_x^2 + P_y^2 \cos^2 \theta + P_z^2 \sin^2 \theta$$

$$\text{OR, } I(\theta) = I_{90} (1 - \Pi \cos^2 \theta)$$

Figure 1

219 >

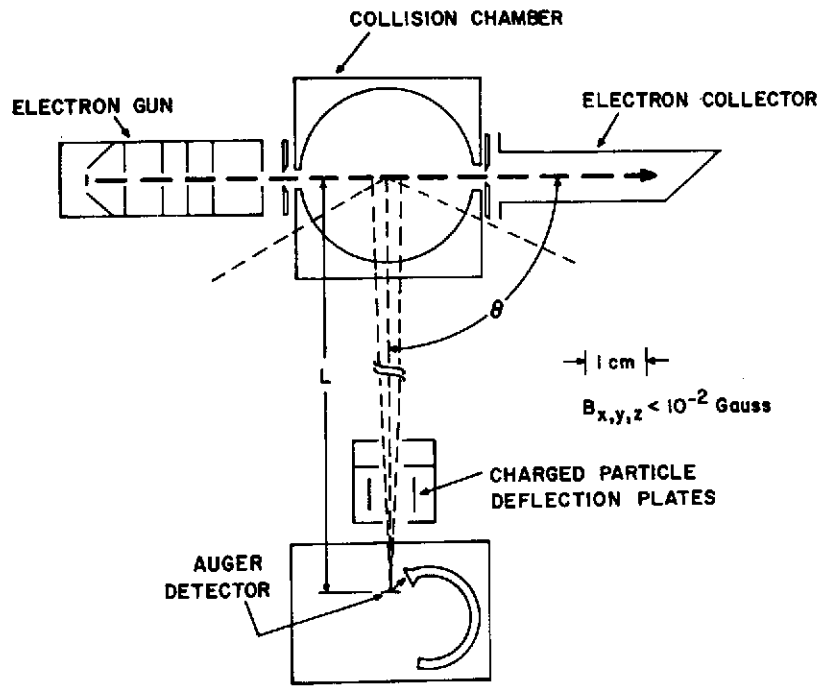


Figure 2

100  
A

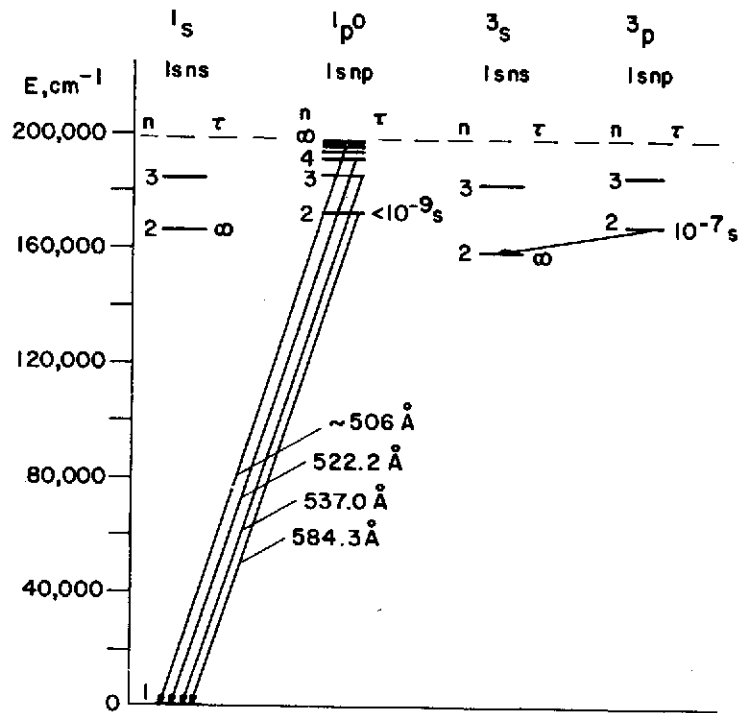


Figure 3

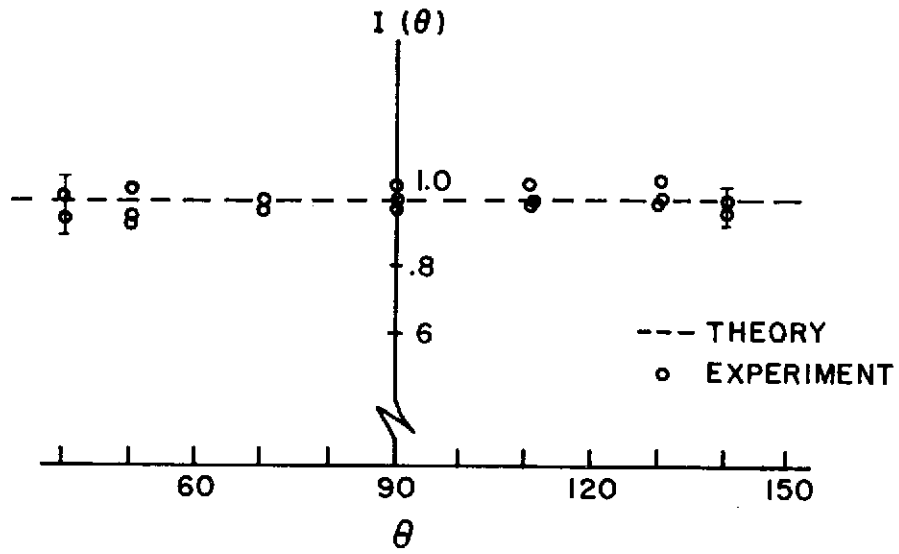


Figure 4

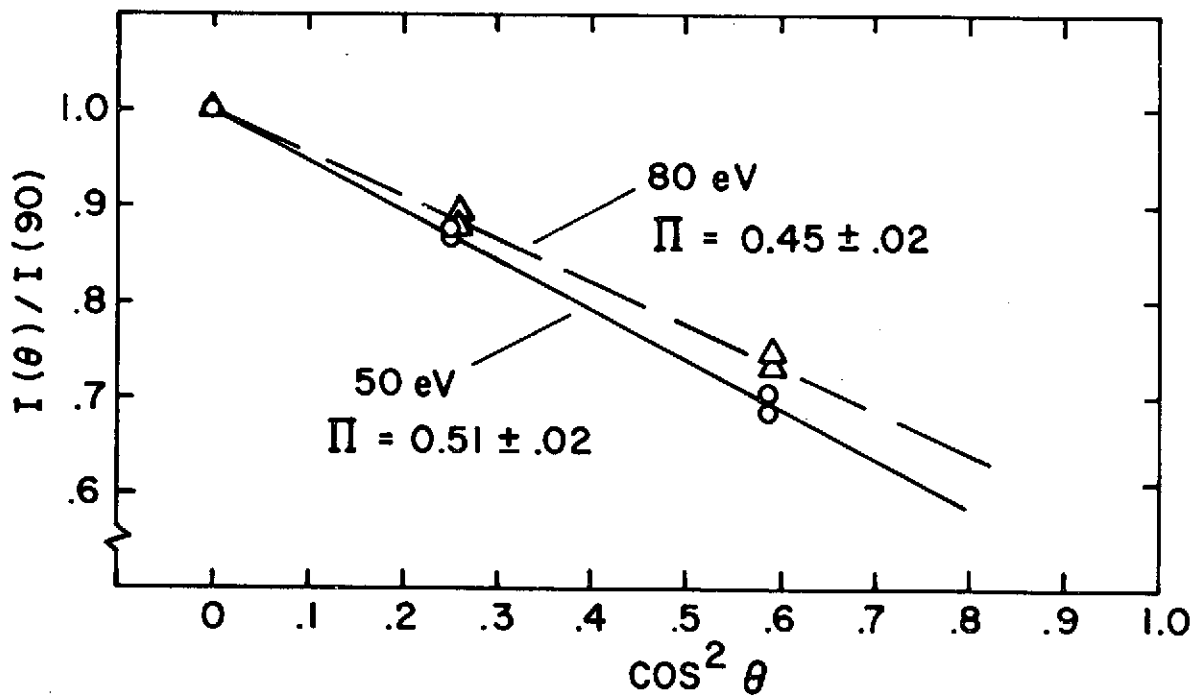


Figure 5

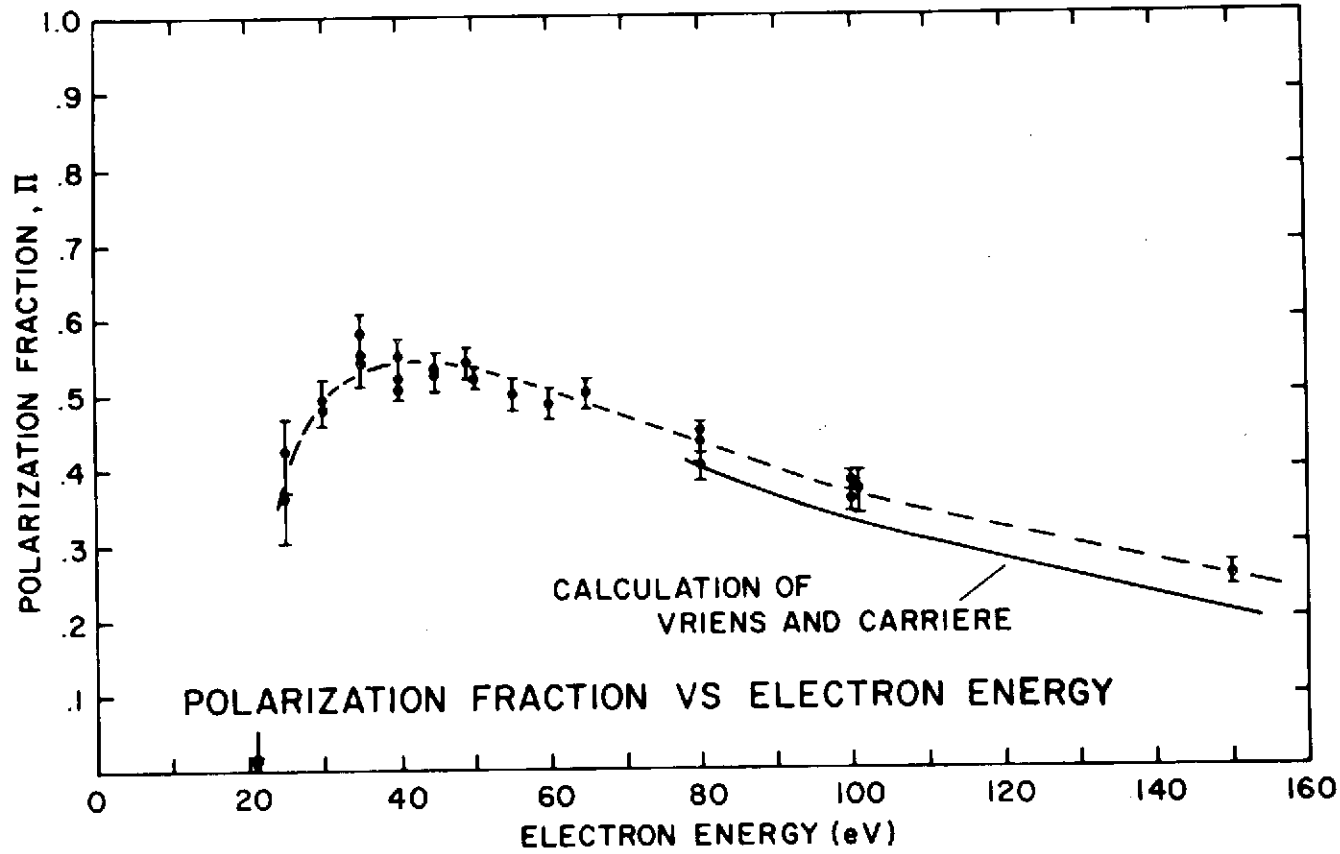


Figure 6



POLARIZATION FRACTION ( $\pi$ ) VS ELECTRON ENERGY  
FOR RESONANCE LINES OF HeI.

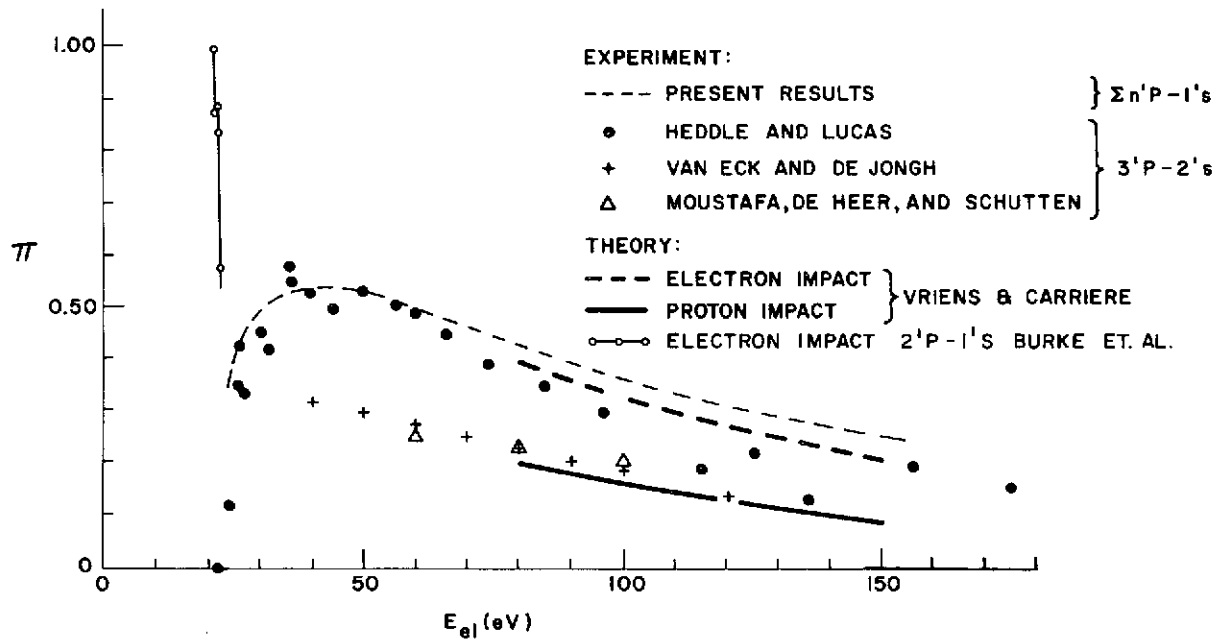


Figure 7